Available online at www.sciencedirect.com
SCIENCE DIRECT®
ELSEVIER
International Journal of Thermal Sciences 42 (2003) 335–342
International Journal of Thermal Sciences
www.elsevier.com/locate/ijts

System-level optimization of the sizes of organs for heat and fluid flow systems

Juan C. Ordóñez, Adrian Bejan *

Department of Mechanical Engineering and Materials Science, Box 90300, Duke University, Durham, NC 27708-0300, USA

Received 4 March 2002; accepted 17 June 2002

Abstract

In this paper we show that the sizes (weights) of heat and fluid flow systems that function on board vehicles such as aircraft can be derived from the maximization of overall (system level) performance. The total weight of the aircraft dictates its fuel requirement. The principle owes its existence to two effects that compete for fuel. Components, power plants and refrigeration plants operate less irreversibly when they are larger. Less irreversibility means less fuel needed for their operation. On the other hand, larger sizes add more to the mass of the aircraft and to the total fuel requirement. This tradeoff pinpoints optimal sizes. The principle is illustrated based on three examples: a power plant the size of which is represented by a heat exchanger, a counterflow heat exchanger without fluid flow irreversibility, and a counterflow heat exchanger with heat transfer and fluid flow irreversibilities. The size optimization principle is applicable to the organs of all flow systems, engineered (e.g., vehicles) and natural (e.g., animals).
© 2002 Éditions scientifiques et médicales Elsevier SAS. All rights reserved.

Keywords: Constructal theory; Thermodynamic optimization; Aircraft; Flight; Size optimization; Organs of animals; Physiology; Zoology

1. Introduction

The total weight of the aircraft dictates its propulsion power requirement, and limits its range. A smaller total weight is better. If the engine can be made to function more efficiently (less irreversibly), then a smaller amount of fuel needs to be installed on board. On the other hand, engine components (e.g., heat exchangers) must be larger to be more efficient, and this tends to increase the total weight of the aircraft. There is a balance between the fuel and engine contributions to the total mass. In agreement with the main line of constructal theory, there is an *optimal way to distribute the imperfection* [1] between the internal and external flows of the aircraft. In this paper we show that from the same principle results the optimal size (mass) of a flow component that functions on board.

The internal flow resistances in this first example are represented by the engine inefficiency, while the external flow resistances are reflected in the power required to sustain the flight. Assume that the total mass M of the aircraft has three components: the mass m_f of the fuel, the mass m_A of the heat transfer surface A employed by all the heat exchangers of all the energy systems on board, and the rest of the aircraft mass (m_0):

$$M = m_f + m_A + m_0 \tag{1}$$

The mass m_0 includes everything: the body, the payload, and all the remaining components of the energy systems installed on board. The fuel mass is time-dependent, $m_f(t)$, as the fuel is consumed gradually during the mission. The other masses (m_A, m_0) are fixed by design. The representative order of magnitude of the fuel mass $m_f(t)$ is the amount present at take-off, $m_{f0} = m_f(0)$. We are interested in the optimal balance between m_A and m_{f0}.

The simplest way to begin (Section 2) is to rule out time-dependent behavior, and examine the instantaneous (per unit time) operation of the aircraft. The instantaneous amount of fuel (m_f) will be compared with the competing mass (m_A), with the objective of minimizing the mechanical power that is required for propulsion (flying).

* Corresponding author.
E-mail address: dalford@duke.edu (A. Bejan).

1290-0729/02/$ – see front matter © 2002 Éditions scientifiques et médicales Elsevier SAS. All rights reserved.
doi:10.1016/S1290-0729(02)00035-2

Nomenclature

a	dimensionless area	
A	area	m^2
c_1	rate of fuel consumption, Eq. (14)	
c_2	fraction of the power required to fly and the twice maximized power extracted from a hot stream	
c_3	group, Eq. (23)	
c_4	group, Eq. (24)	
c_5	group, Eq. (38)	
c_p	specific heat at constant pressure	$J\cdot kg^{-1}\cdot K^{-1}$
C_D	drag coefficient	
D	linear dimension of the flying body	m
f	fouling factor	
F	drag force	N
F_v	function, Eq. (10)	
g	gravity	$m\cdot s^{-2}$
G_v	factor, Eq. (13)	
L	length	m
$\dot{m}$	mass flow rate	$kg\cdot s^{-1}$
m	mass	kg
M	total mass of aircraft	kg
N_S	entropy generation number, Eq. (39)	
N_{tu}	number of heat transfer units	
p	perimeter	m
P	pressure	Pa
$\dot{Q}$	heat transfer rate	W
R	ideal gas constant	$J\cdot kg^{-1}\cdot K^{-1}$
$\dot{S}_{gen}$	entropy generated	$W\cdot K^{-1}$
St	Stanton number	
t	time	s
T	temperature	K
U	overall heat transfer coefficient	$W\cdot m^{-2}\cdot K^{-1}$
V	velocity	$m\cdot s^{-1}$
$\dot{W}$	power	W

Greek symbols

δ	thickness of the heat transfer wall	m
ΔT	stream to stream temperature difference	K
ΔP	pressure drop	Pa
ε	heat exchanger effectiveness	
θ	group, Eq. (40)	
μ	viscosity	$kg\cdot(sm)^{-1}$
τ	dimensionless temperature, Eq. (35)	

Subscripts

a	air
A	heat transfer surface
b	flying body
f	fuel
f_0	fuel at time $t = 0$
H	hot stream
L	low temperature, collecting stream
min	minimum
mm	maximized twice
opt	optimal
out	exit
rev	reversible
s	surface
x	horizontal component of the exit velocity
0	rest of aircraft
0	ambient
1, 2	sides of the heat transfer surface

Superscript

$(\tilde{\ })$	dimensionless variables, Eqs. (19), (23) and (35)

2. Power required to sustain flight

As shown in Ref. [1], the most basic features and needs of powered flight are retained in the simple model of Fig. 1. The flying body of mass M has the single linear dimension D, density ρ_b, and horizontal speed V relative to the surrounding air. The air density ρ_a is much smaller than ρ_b. This leads to the global requirement that the net vertical body force $Mg \sim \rho_b D^3 g$ must be supported by other forces. The generation of the latter is achieved through the relative motion called flight.

Consider the conservation of mass and momentum in the control volume occupied by the flying body and the immediately close fluid regions affected by relative motion. In the steady state, an air stream of mass flow rate $\dot{m} \sim \rho_a D^2 V$ enters the control volume and the same stream exits ($\dot{m} \sim \rho_a D_{out}^2 V_{out}$) . The exit velocity V_{out} must have a vertical component V_{down} in order to develop a vertical flow of momentum to support the body force:

$$V_{out} = \left(V_x^2 + V_{down}^2\right)^{1/2} \tag{2}$$

The vertical momentum balance is $\rho_b D^3 g \sim \dot{m} V_{down}$, or

$$V_{down} \sim \frac{\rho_b g D}{\rho_a V} \tag{3}$$

The conservation of horizontal momentum is the statement that the momentum generated by the outflow ($\dot{m} V_x$) must balance the retarding forces associated with momentum inflow ($\dot{m} V$) and drag (F):

$$\dot{m} V_x \sim \dot{m} V + F \tag{4}$$

The drag force F is of order of $C_D D^2 \rho_a V^2$, where D^2 is the scale of the body cross section. The drag coefficient C_D is a relatively constant number of the order of 1, because the Reynolds number ($\rho_a V D/\mu_a$) is greater than the order of 10^2 (e.g., Ref. [2, p. 325]). This means that the ratio

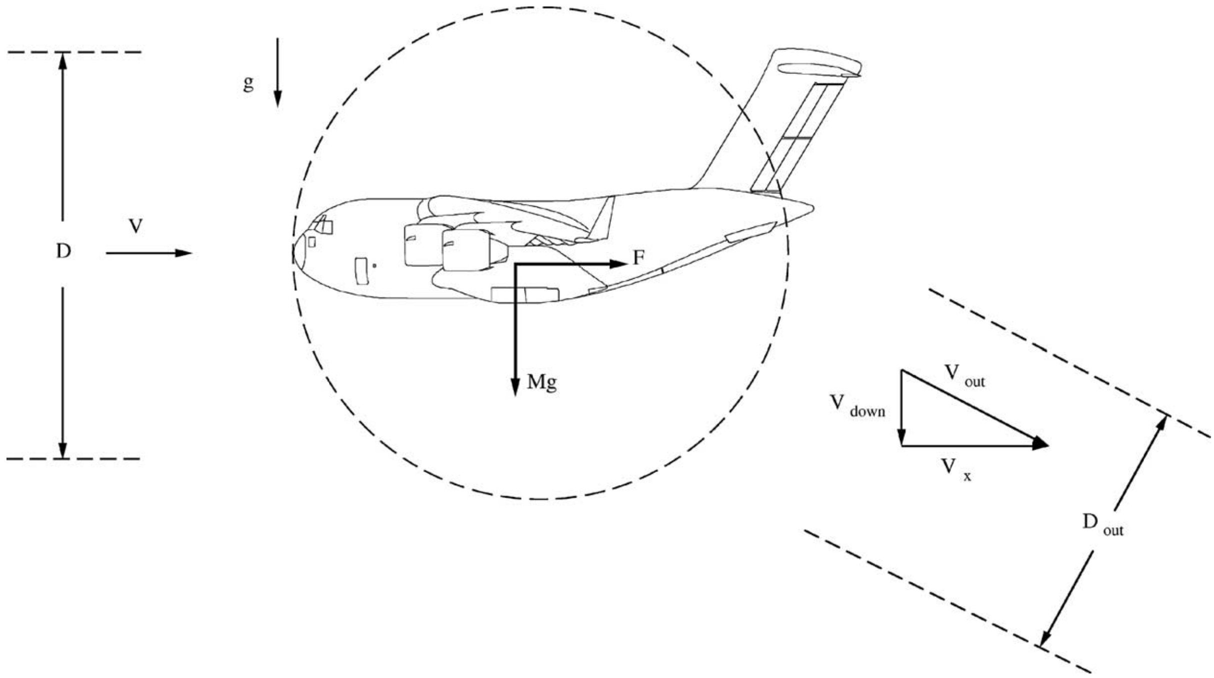

Fig. 1. Simple model and interactions of a flying body.

$F/\dot{m}$ scales as V. In summary, the flying system must spend exergy or mechanical power ($\dot{W}$) in order to increase the kinetic energy of the air stream from the inlet ($\dot{m}V^2/2$) to the outlet ($\dot{m}V_{\text{out}}^2/2$):

$$\dot{W} \sim \frac{1}{2}\dot{m}\left(V_{\text{out}}^2 - V^2\right) \tag{5}$$

In an aircraft $\dot{W}$ is produced by the power plant installed on board: $\dot{W}$ is drawn from the chemical exergy of the consumed fuel.

By using approximations (2)–(4), approximating $V_x^2 \sim (V + F/\dot{m})^2 \sim V^2 + 2VF/\dot{m}$, and neglecting all the factors of the order of 1, we can eliminate V_{down} and rewrite approximation (5) as

$$\dot{W} \sim \frac{\rho_b^2 g^2 D^4}{\rho_a V} + \rho_a D^2 V^3 \tag{6}$$

This two-term expression shows the power that is required for maintaining the body in the air (the first term) and overcoming the drag (the second term). Changes in the flying speed induce changes of opposing signs in the two terms. Power function (6) has a minimum with respect to V [1,3,4],

$$V_{\text{opt}} \sim 3^{-1/4}\left(\frac{\rho_b}{\rho_a} g D\right)^{1/2} \tag{7}$$

$$\dot{W}_{\min} \sim \frac{4\rho_b^{3/2} g^{3/2} \mathrm{D}^{7/2}}{3^{3/4}\rho_a^{1/2}} \tag{8}$$

At this optimum the power spent on lifting the body is three times larger than the power needed to overcome the drag. Here we have an example of optimal allocation, or optimal partition, which is a common occurrence in thermodynamic optimization and constructal theory [1,5]. When the flying speed is significantly less than the optimal, the power requirement is dominated by the need to hold (lift repeatedly) the body in the air. In the opposite extreme the power is spent mainly on overcoming drag.

It is reasonable to allow the cruising speed V to vary, however, its order of magnitude will be dictated by the V_{opt} scale. To emphasize this, in Eq. (6) we replace V by $(V/V_{\text{opt}})V_{\text{opt}}$, where $V/V_{\text{opt}} \sim 1$, and V_{opt} is furnished by Eq. (7). The result is

$$\dot{W} \sim \frac{\rho_b^{3/2} g^{3/2} D^{7/2}}{\rho_a^{1/2}} F_v \tag{9}$$

where

$$F_v = 3^{1/4}\frac{V_{\text{opt}}}{V} + 3^{-3/4}\left(\frac{V}{V_{\text{opt}}}\right)^3 \tag{10}$$

The function F_v is minimum when $V = V_{\text{opt}}$. The value of F_v is of order 1 when V is comparable with V_{opt}. The alternative to Eq. (9) is to replace D in terms of M, by using the scaling law $M \sim \rho_b D^3$:

$$\dot{W} \sim \rho_a^{-1/2}\rho_b^{1/3} g^{3/2} M^{7/6} F_v \tag{11}$$

This form shows that the power required for flying is almost proportional to the total mass of the aircraft. We show this more clearly by dividing Eq. (11) by the speed V,

$$\dot{W} \sim G_v M g V \tag{12}$$

where

$$G_v = 3^{1/2}\left(\frac{V_{\text{opt}}}{V}\right)^2 + 3^{-1/2}\left(\frac{V}{V_{\text{opt}}}\right)^2 \tag{13}$$

The factor G_v is approximately 2 when V is of the same order as V_{opt}. In conclusion, the flying power requirement is proportional to the total mass of the aircraft. In the following sections we ask how the flow components of the aircraft contribute to M, and how their sizes can be selected such that the overall consumption of fuel is minimized.

3. Larger power systems are more efficient

Eq. (12) with $G_v \sim 2$ shows that a smaller M is desirable from the point of view of minimizing the fuel consumed for the mission. A smaller total mass (M) demands a smaller amount of fuel m_f, and, necessarily, a more efficient power plant. Higher thermodynamic efficiencies go with larger sizes, in both power plants and refrigeration plants [6,7], and this works against the spirit of minimizing M and $\dot{W}$. The identification of the relationship between improved thermodynamic performance and increased size (mass) is essential to the problem of determining the optimal size of components in a complex energy system.

Assume that the steady flight described in Fig. 1 is powered by the burning of a steady stream of fuel of flow rate $\dot{m}_f$. Assume further that the combustion occurs in an adiabatic chamber situated upstream (to the left) of Fig. 2. Combustion produces a gaseous stream of combustion products of flow rate $\dot{m}$ and adiabatic flame temperature T_H. Parameters $\dot{m}$ and T_H are known as soon as the fuel flow rate and the combustion reactants are specified. The flow rate of products is proportional to the rate of fuel consumption,

$$\frac{\dot{m}_f}{\dot{m}} = c_1 < 1 \tag{14}$$

The problem of the maximum power that can be extracted from the stream of hot gases ($\dot{m}$, T_H) was treated in Ref. [8]. With reference to Fig. 2, it was assumed that the interface between the hot stream and the rest of the power plant is a heat transfer surface of finite size A and overall heat transfer coefficient U. The rest of the power plant is modeled as reversible, and is represented by the lower white trapezoid in Fig. 2. The temperature T_0 represents the ambient. The length L traveled by the hot stream is proportional to the heat transfer area, $A = pL$, where p is the heat transfer area per unit of flow path length.

The power producing compartment is a succession of many infinitesimal reversible compartments of the kind shown in the center of Fig. 2. The infinitesimal power output is $\mathrm{d}\dot{W}_{rev} = [1 - T_0/T_s(x)]\,\mathrm{d}\dot{Q}_H$, where the temperature is plotted on the vertical, and $\mathrm{d}\dot{Q}_H = \dot{m}c_p\,\mathrm{d}T$. The heat transfer through the heat exchanger area is $\mathrm{d}\dot{Q}_H = [T(x) - T_s(x)]Up\,\mathrm{d}x$. Combining these equations and integrating from $x = 0$ to $x = L = A/p$ while treating U as a constant we arrive at the finite-area constraint and the total power output:

$$\int_{T_{out}}^{T_H} \frac{\mathrm{d}T}{T - T_s} = \frac{UA}{\dot{m}c_p} = N_{tu} \tag{15}$$

$$\dot{W}_{rev} = \int_{T_{out}}^{T_H} \left(1 - \frac{T_0}{T_s}\right)\dot{m}c_p\,\mathrm{d}T \tag{16}$$

There are two degrees of freedom in the maximization of the power extraction rate $\dot{W}_{rev}$: the shape of the surface temperature function $T_s(x)$, and the place of this function on the temperature scale (i.e., closer to T_H or T_0). The second degree of freedom is alternately represented by the value of the exhaust temperature T_{out}.

Maximization of $\dot{W}_{rev}$ is achieved when the optimal hot-stream temperature distribution $T(x)$ is exponential in x, and so is the temperature $T_s(x)$ along the hot end of the system that converts the heating into mechanical power. At any x, the temperature difference across the heat exchanger is proportional to the local absolute temperature. The optimal solution can be implemented in practice by using a single-phase stream in place of the $T_s(x)$ surface: this stream runs

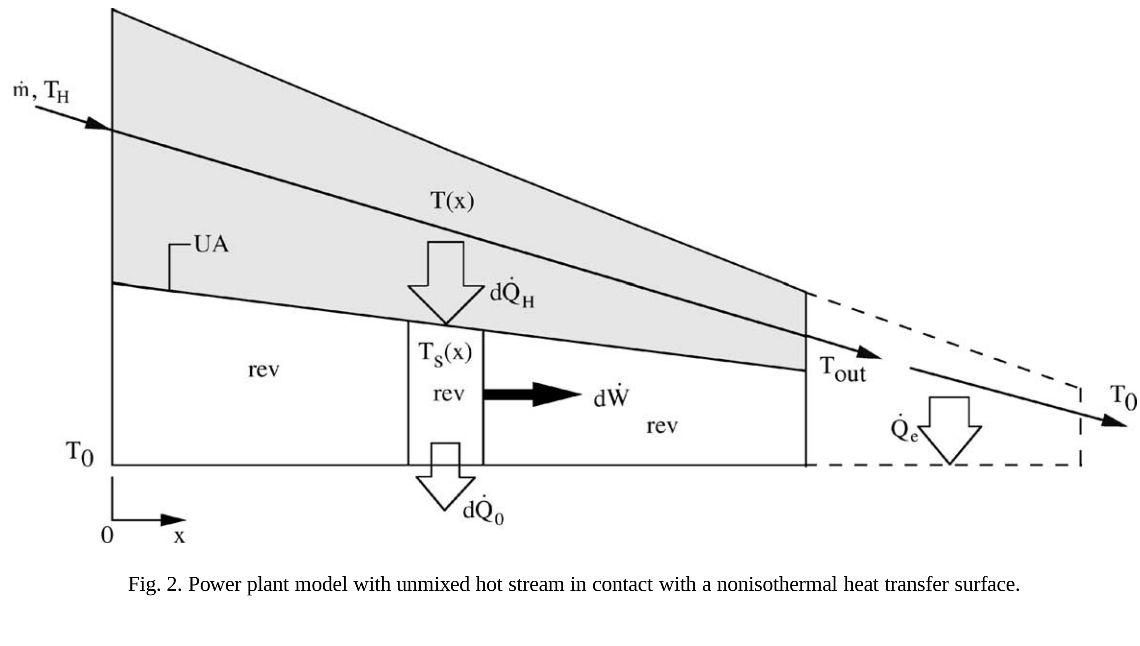

Fig. 2. Power plant model with unmixed hot stream in contact with a nonisothermal heat transfer surface.

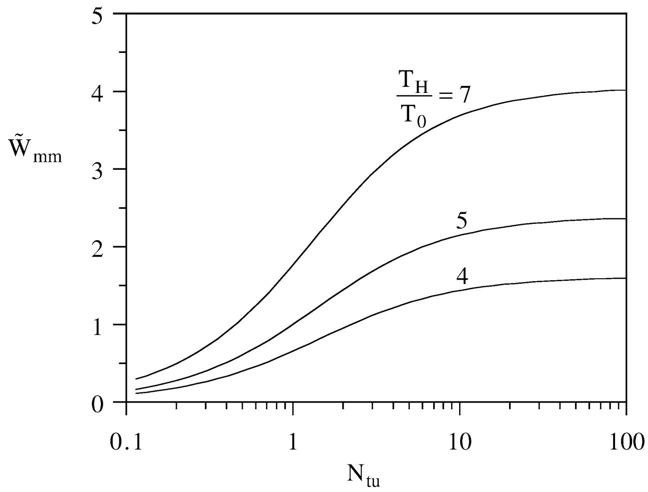

Fig. 3. The maximum power extracted from a stream of hot gas, by using a heat transfer surface of finite size.

in counterflow relative to the hot stream $\dot{m}$. The counterflow imbalance (the ratio between the capacity flow rates of the two streams) is the result of thermodynamic optimization. The production of maximum $\dot{W}_{\rm rev}$ is represented by the equations [8]

$$\frac{\dot{W}_{\rm mm}}{\dot{m}c_{\rm p}T_0} = \frac{T_{\rm H}}{T_0} - \frac{T_{\rm out}}{T_0} - \left(\frac{T_{\rm out}}{T_0}\right)^{1/2} \ln \frac{T_{\rm H}}{T_{\rm out}} \tag{17}$$

$$\frac{T_{\rm out}}{T_0}\left(1 - \frac{1}{N_{\rm tu}} \ln \frac{T_{\rm H}}{T_{\rm out}}\right)^2 = 1 \tag{18}$$

from which $T_{\rm out}$ can be eliminated to obtain $\dot{W}_{\rm mm}$ as a function of imposed parameters $(\dot{m}, T_{\rm H}, T_0)$. The subscript mm indicates that $\dot{W}_{\rm rev}$ was maximized twice, with respect to the $T_{\rm s}(x)$ function and $T_{\rm out}$. The result of combining Eqs. (17) and (18) is the dimensionless function

$$\frac{\dot{W}_{\rm mm}}{\dot{m}c_{\rm p}T_0} = \widetilde{W}_{\rm mm}\left(N_{\rm tu}, \frac{T_{\rm H}}{T_0}\right) \tag{19}$$

which is presented in Fig. 3. The power output is larger when the heat transfer area ($N_{\rm tu}$) is greater. Larger power plants are more efficient. A similar trend is exhibited by refrigeration and liquefaction plants, where the second law efficiencies of existing plants increase as capacities (refrigeration loads) increase [6,7].

4. Optimal area size, and optimal amount of fuel

The purpose of the power produced by the engine is to provide the power necessary for sustaining the flight and all the other energy-system requirements on board. Consequently, the estimate shown on the right side of approximation (11) is a significant fraction ($c_2 \lesssim 1$) of the $\dot{W}_{\rm mm}$ estimate provided by Eq. (19),

$$\rho_{\rm a}^{-1/2}\rho_{\rm b}^{1/3}g^{3/2}M^{7/6}F_{\rm v} = c_2\dot{m}c_{\rm p}T_0\widetilde{W}_{\rm mm} \tag{20}$$

The hot-gas flow rate $\dot{m}$ is related to the fuel rate $\dot{m}_{\rm f}$ by Eq. (14). If the amount of fuel is $m_{\rm f}$, and the flight time is t, then

$$\dot{m}_{\rm f} = m_{\rm f}/t \tag{21}$$

Substituting $\dot{m} = m_{\rm f}/(c_1 t)$ and Eq. (1) into Eq. (20), we obtain

$$\frac{c_1}{c_2}c_3F_{\rm v}\left(1 + \tilde{m}_{\rm A} + \tilde{m}_{\rm f}\right)^{7/6} = \tilde{m}_{\rm f}\widetilde{W}_{\rm mm} \tag{22}$$

where

$$c_3 = \frac{\rho_{\rm b}^{1/3}g^{3/2}m_0^{1/6}t}{\rho_{\rm a}^{1/2}c_{\rm p}T_0}$$
$$\tilde{m}_{\rm A} = m_{\rm A}/m_0 \tag{23}$$
$$\tilde{m}_{\rm f} = m_{\rm f}/m_0$$

On the right side of Eq. (22), $\widetilde{W}_{\rm mm}$ is a function of $T_{\rm H}/T_0$ (fixed) and $N_{\rm tu}$ (variable). The latter is related to the $m_{\rm A}/m_{\rm f}$ ratio in the following way. The mass of the heat transfer hardware is $m_{\rm A} = A\delta\rho_{\rm A}$, where δ and $\rho_{\rm A}$ are the thickness of the heat transfer wall and the density of the wall material. Substituting $A = m_{\rm A}/(\delta\rho_{\rm A})$ and $\dot{m} = m_{\rm f}/(c_1 t)$ into $N_{\rm tu} = UA/\dot{m}c_{\rm p}$ we obtain

$$N_{\rm tu} = c_4\frac{\tilde{m}_{\rm A}}{\tilde{m}_{\rm f}}, \qquad c_4 = \frac{c_1\tau U}{\delta\rho_{\rm A}c_{\rm p}} \tag{24}$$

Eq. (22), Fig. 3 and Eq. (24) establish $\tilde{m}_{\rm A}$ as a function of $\tilde{m}_{\rm f}$. A certain size ($\tilde{m}_{\rm A}$) is needed in order to perform the flying mission using a certain amount of fuel ($\tilde{m}_{\rm f}$). The relationship between these two masses is illustrated in Fig. 4, which was drawn by assuming $c_1 = 0.0148$, $F_{\rm v} = 1$, $c_3 = 105.1$ and $c_4 = 283.1$. The value of c_1 corresponds to a fuel/air ratio of 0.015. The value of c_3 is based on assuming $\rho_{\rm a} = 0.414\ {\rm kg{\cdot}m^{-3}}$, $T_0 = 223$ K, $\rho_{\rm b} \cong 10^2\ {\rm kg{\cdot}m^{-3}}$, $c_{\rm p} = 1157\ {\rm J{\cdot}kg^{-1}{\cdot}K^{-1}}$, $m_0 = 10^5$ kg and $t = 5$ h. The values selected for T_0 and $\rho_{\rm a}$ correspond to the standard atmosphere at an altitude of 10 km [9]. In addition, we fixed the temperature ratio $T_{\rm H}/T_0 = 7$. The values of c_1 and $T_{\rm H}/T_0$ are representative of kerosene fuel combustion [9]. The constant $c_{\rm p}$ value is the one normally used for the hot-end gas stream [9]. The c_4 value was calculated by assuming $c_1 = 0.0148$, $\delta = 0.3$ mm, $\rho_{\rm A} = 2707\ {\rm kg{\cdot}m^{-3}}$ (aluminum) and $U = 10^3\ {\rm W{\cdot}m^{-2}{\cdot}K^{-1}}$.

Fig. 4 shows that the relation between $\tilde{m}_{\rm A}$ and $\tilde{m}_{\rm f}$ has the special property that at sufficiently large $\tilde{m}_{\rm f}$ values the function $\tilde{m}_{\rm A}(\tilde{m}_{\rm f})$ is double-valued. For a given rate of propulsive power (c_2), the amount of fuel must exceed a certain minimum level for the design to be viable. In the numerical case of Fig. 4, the minimum $\tilde{m}_{\rm f}$ is of order 1, which means that the minimum fuel mass is comparable with the mass of the rest of the aircraft (m_0). At this stage we do not have a rational or intuitive basis on which to discard the dashed-line portions of the curves. Their place in the optimization results continues to be indicated by dashed lines (Figs. 4 and 5).

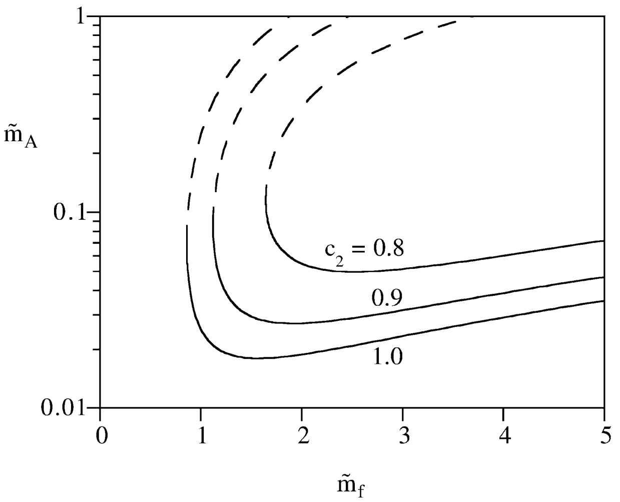

Fig. 4. The relation between area size and amount of fuel.

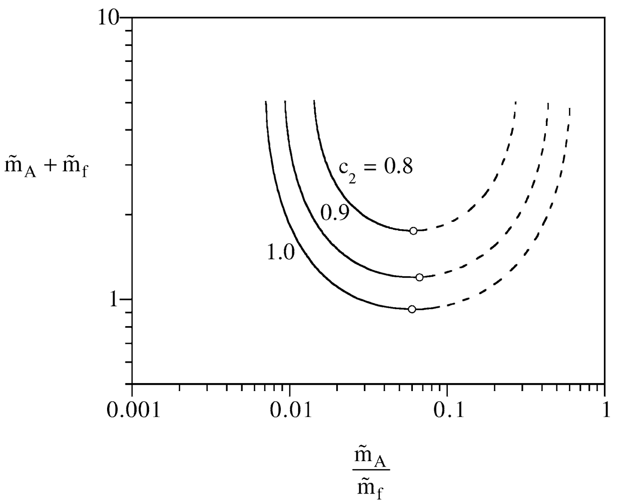

Fig. 5. The minimization of the total mass with respect to the mass allocation ratio.

Optimization means to minimize the flying power requirement (the left side of Eq. (22)), the total mass $(1+\tilde{m}_A+\tilde{m}_f)$, or the sum $(\tilde{m}_A+\tilde{m}_f)$. The variation of $(\tilde{m}_A+\tilde{m}_f)$ with respect to the mass allocation ratio $\tilde{m}_A/\tilde{m}_f$ is shown in Fig. 5. There is an optimal area size, and a corresponding amount of fuel, such that the overall performance of the aircraft is maximized. The minima of $(\tilde{m}_A+\tilde{m}_f)$ fall on the solid portions of the curves, indicating that the trade-off between $\tilde{m}_f$ and $\tilde{m}_A$ is associated with the descending portions of the $\tilde{m}_A(\tilde{m}_f)$ curves shown in Fig. 4. The optimal ratio $\tilde{m}_A/\tilde{m}_f$ is approximately 0.06, and is relatively independent of the assumed power transmission factor c_2. The minimum of the group ($\tilde{m}_A+\tilde{m}_f$) is of order 1, because $\tilde{m}_f \gg \tilde{m}_A$ and $\tilde{m}_f \sim 1$. Comparing Fig. 5 with Fig. 4, we conclude that the minimal $\tilde{m}_f$ values identified in Fig. 4 are in the range where the group ($\tilde{m}_A+\tilde{m}_f$) reaches its minimum.

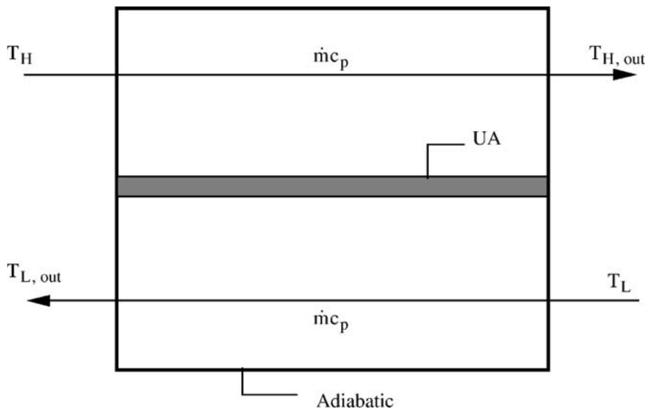

Fig. 6. Balanced counterflow heat exchanger.

5. Optimal heat exchanger size

As a second example of the optimization of the size of a component, consider the balanced counterflow heat exchanger shown in Fig. 6. By optimal size, we mean the size that minimizes the sum of lost power due to irreversibilities and the power invested in carrying the heat exchanger on the aircraft.

We use the simplest heat exchanger description, where only the irreversibilities associated with temperature differences are taken into account. The heat transfer performance is described by the effectiveness-N_{tu} formulas,

$$\varepsilon = \frac{T_H - T_{H,out}}{T_H - T_L} = \frac{T_{L,out} - T_L}{T_H - T_L} = \frac{N_{tu}}{1+N_{tu}} \tag{25}$$

from which the two outlet temperatures can be calculated,

$$T_{H,out} = T_H(1-\varepsilon) + \varepsilon T_L \tag{26}$$

$$T_{L,out} = T_L + \varepsilon(T_H - T_L) \tag{27}$$

The degree of thermodynamic imperfection of the heat exchange process is indicated by the entropy generation rate,

$$\dot{S}_{gen,\Delta T} = \dot{m}c_p \ln\frac{T_{H,out}}{T_H} + \dot{m}c_p \ln\frac{T_{L,out}}{T_L} \tag{28}$$

The corresponding rate of exergy destruction is [6]

$$\dot{W}_{lost,\Delta T} = T_0 \dot{S}_{gen} \tag{29}$$

This exergy was originally generated by burning fuel. Equation (29) can be rewritten using Eqs. (25)–(28),

$$\begin{aligned}\dot{W}_{lost,\Delta T} = {}& \dot{m}c_p T_0 \left\{ \ln\left[\frac{N_{tu}}{1+N_{tu}}\left(\frac{1}{N_{tu}} + \frac{T_L}{T_H}\right)\right]\right. \\ &\left. + \ln\left[1 + \frac{N_{tu}}{N_{tu}+1}\left(\frac{T_H}{T_L} - 1\right)\right]\right\}\end{aligned} \tag{30}$$

In summary, Eq. (30) indicates the power lost due to temperature differences, as a function of the heat exchanger size (N_{tu}).

The minimum work required to carry a heat exchanger of mass m on board during a flight at near-optimal speed

V is proportional to $2mgL$, where L is the distance traveled (Ref. [1, p. 239]). Per unit time, we have

$$\dot{W} \simeq 2mgV \tag{31}$$

in agreement with Eq. (12). The optimal or near-optimal speed V is dictated by the total mass of the aircraft (M). We assume that V is independent of the heat exchanger mass (m), because m is a small fraction of the total aircraft mass. The mass of the heat exchanger is proportional to N_{tu},

$$N_{\mathrm{tu}} = \frac{Um}{\dot{m}c_{\mathrm{p}}\delta\rho_{\mathrm{A}}} \tag{32}$$

so that Eq. (31) becomes

$$\dot{W} \simeq 2gV\dot{m}c_{\mathrm{p}}\delta\rho_{\mathrm{A}}N_{\mathrm{tu}}/\mathrm{U} \tag{33}$$

Next, we assume that the heat transfer duty of the heat exchanger is fixed [10],

$$\begin{aligned}\dot{Q} &= \dot{m}c_{\mathrm{p}}(T_{\mathrm{H}} - T_{\mathrm{H,out}}) \\ &= \dot{m}c_{\mathrm{p}}(T_{\mathrm{L,out}} - T_{\mathrm{L}}) = \dot{m}c_{\mathrm{p}}\varepsilon(T_{\mathrm{H}} - T_{\mathrm{L}})\end{aligned} \tag{34}$$

Using the nondimensional groups,

$$\widetilde{W} = \frac{\dot{W}}{\dot{Q}}, \qquad \tau = \frac{T}{T_{\mathrm{L}}} \tag{35}$$

we can rewrite Eq. (30) as

$$\begin{aligned}&\widetilde{W}_{\mathrm{lost},\Delta T} \\ &\quad = \frac{1+N_{\mathrm{tu}}}{N_{\mathrm{tu}}(\tau_{\mathrm{H}} - \tau_{\mathrm{L}})}\left\{\ln\left[\frac{N_{\mathrm{tu}}}{1+N_{\mathrm{tu}}}\left(\frac{1}{N_{\mathrm{tu}}} + \frac{\tau_{\mathrm{L}}}{\tau_{\mathrm{H}}}\right)\right]\right. \\ &\qquad \left. + \ln\left[1 + \frac{N_{\mathrm{tu}}}{N_{\mathrm{tu}}+1}\left(\frac{\tau_{\mathrm{H}}}{\tau_{\mathrm{L}}} - 1\right)\right]\right\}\end{aligned} \tag{36}$$

which in the limit $N_{\mathrm{tu}} \to 0$ has the property

$$\widetilde{W}_{\mathrm{lost},\Delta T} = \frac{\tau_{\mathrm{H}} - \tau_{\mathrm{L}}}{\tau_{\mathrm{H}}\tau_{\mathrm{L}}} \tag{37}$$

Eq. (33) becomes

$$\widetilde{W} = \frac{c_5}{\tau_{\mathrm{H}} - \tau_{\mathrm{L}}}(N_{\mathrm{tu}} + 1), \qquad c_5 = \frac{2gV\delta V_{\mathrm{A}}}{UT_0} \tag{38}$$

For example, $c_5 = 1.18 \times 10^{-5}$ when $\delta = 0.3$ mm, $\rho_{\mathrm{A}} = 2707$ kg·m^{-3}, $U = 10^3$ W·m^{-2}·K^{-1}, $T_0 = 298$ K, and $V = 800$ km·h^{-1}.

The objective is to minimize the sum $\widetilde{W}_{\mathrm{lost},\Delta T} + \widetilde{W}$. Fig. 7 shows the emergence of an optimal heat exchanger size, N_{tu}. The exergy destroyed by the heat exchanger decreases as the size increases. At the same time, the fuel exergy destroyed for the purpose of flying the heat exchanger mass increases. The balance between these two effects yields the optimal size, which is reported in Fig. 8 as a function of τ_{H} and c_5. The optimal N_{tu} is proportional to $c_5^{-1/2}$, and increases weakly with τ_{H}.

The optimization can be refined by taking into account the irreversibility due to fluid flow. For example, it was shown that in the ideal heat exchanger limit (small ΔT and ΔP), the entropy generation rate subject to area constraint and fixed Reynolds number is [6]

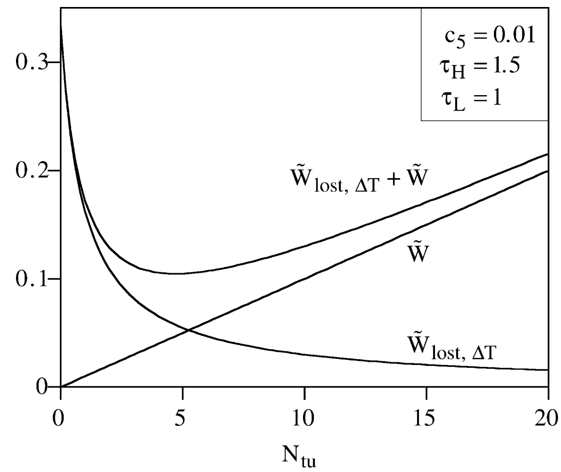

Fig. 7. The optimization of the size of the counterflow heat exchanger.

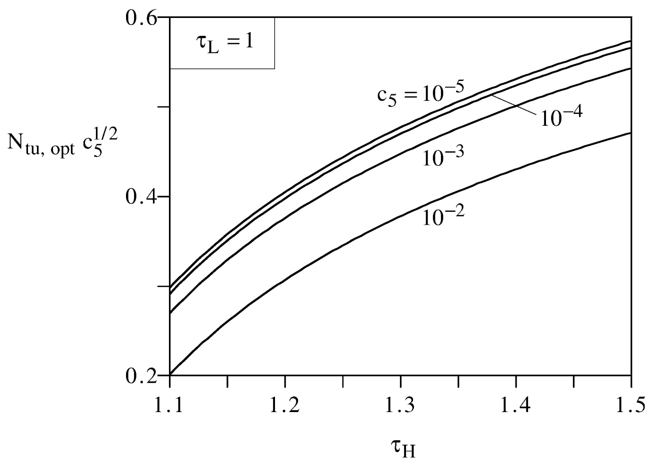

Fig. 8. The optimal size of the counterflow heat exchanger.

$$N_{S,\min} = \frac{\dot{S}_{\mathrm{gen}}}{\dot{m}c_{\mathrm{p}}} = \left[\frac{256\theta^6(R/c_{\mathrm{p}})f_1}{27a_1^2St_1^3}\right]^{1/4} + \left[\frac{256\theta^6(R/c_{\mathrm{p}})f_2}{27a_2^2St_2^3}\right]^{1/4} \tag{39}$$

Subscripts 1 and 2 refer to the two sides of the heat transfer surface, while St represents the Stanton number, f the friction factor, and θ is a dimensionless parameter fixed by T_1 and T_2:

$$\theta^2 = \frac{(T_2 - T_1)^2}{T_1T_2} \tag{40}$$

The dimensionless areas swept by each stream are

$$a_{1,2} = \frac{A_{1,2}}{\dot{m}}(2\rho P_{1,2})^{1/2} \tag{41}$$

If we consider the simple case where $A_1 = A_2 = A/2$, $P_1 = P_2$ and the flow conditions

$$\frac{f_1}{a_1^2St_1^3} \cong \frac{f_2}{a_2^2St_2^3} = \frac{f}{a^2St^3} \tag{42}$$

then the exergy lost because of ΔTs and ΔPs is

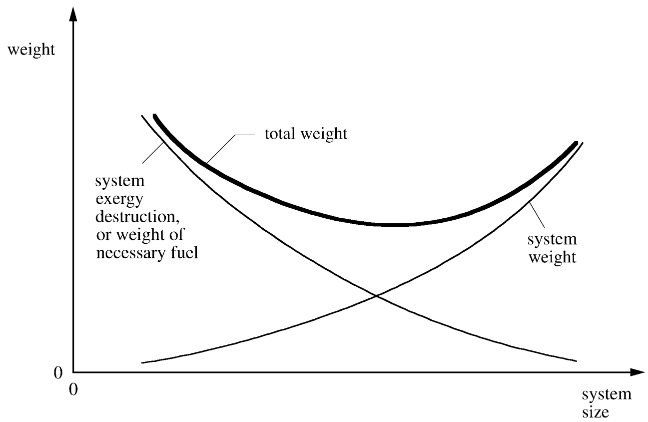

Fig. 9. The minimization of the total weight associated with a flow system: The weight of the system plus the weight of the fuel installed on board to account for the exergy destroyed in the system.

$$\widetilde{W}_{\mathrm{lost},\Delta T,\Delta P} = 2\left[\frac{256\theta^6(R/c_\mathrm{p})f}{27St^3}\right]^{1/4}\left[\frac{U}{(2\rho P)^{1/2}c_\mathrm{p}N_\mathrm{tu}}\right]^{1/2} \tag{43}$$

This quantity varies as $N_\mathrm{tu}^{-1/2}$, therefore, the thermodynamic goodness of the heat exchanger is enhanced by investing more area in the design. But, as in the previous case, the exergy required in order to carry the heat exchanger on board increases as N_tu increases, Eq. (33). The behavior is qualitatively the same as in Fig. 7. From this tradeoff one can deduce the optimal N_tu, i.e., the optimal heat exchanger size.

6. Conclusion: Optimum sizes for the "organs" of vehicles and animals

The main idea proposed in this paper is that the sizes of components can be optimized, such that the aggregate system—the vehicle—performs at the highest level possible. We illustrated this by analyzing energy flow systems that function on aircraft. To begin with, the total weight of the aircraft dictates its power requirement, and limits its range. A small total weight is better. Smaller components in every subsystem of the aircraft appear to be preferable.

There is another trend that contradicts the drive toward smaller sizes. Power and refrigeration systems and their components function less efficiently when their sizes decrease. Their various flow resistances increase when sizes decrease. In a heat exchanger, for example, the heat-transfer area and the fluid-flow cross-sections decrease when the total mass and volume decrease. Larger flow resistances lead to higher rates of exergy destruction and, globally, to the requirement of installing more fuel on board. More fuel means more weight.

This conflict, which was analyzed in several examples in the paper, is summarized in Fig. 9. The total installed weight of a system is the sum of the actual weight of the system and the weight of the fuel that must be used in order to produce the exergy that is ultimately destroyed by the system. The total weight installed on board has a minimum, which identifies the optimal size of the system. This tradeoff is fundamental: we can expect it in every flow system, in every vehicle and living system (e.g., animal), no matter how complex.

Acknowledgements

The authors acknowledge with gratitude the guidance provided in this research project by Mr. David L. Siems of the Boeing Corporation. This material is based upon work supported by the Air Force Office of Scientific Research under Contract No. F49620-98-C-0007. Any opinions, findings and conclusions or recommendations are those of the authors and do not necessarily reflect the views of the Air Force Office of Scientific Research. Juan C. Ordóñez acknowledges with gratitude the support of the Energy and Thermodynamics Group at Pontificia Bolivariana University (Colombia).

References

[1] A. Bejan, Shape and Structure, from Engineering to Nature, Cambridge University Press, Cambridge, UK, 2000.
[2] A. Bejan, Convection Heat Transfer, 2nd Edition, Wiley, New York, 1995.
[3] C.J. Pennycuick, Animal Flight, Edward Arnold, London, UK, 1972.
[4] H. Tennekes, The Simple Science of Flight, MIT Press, Cambridge, MA, 1986.
[5] M. Feidt, Thermodynamique et Optimisation Énergetique des Systèmes et Procedés, Technique et Documentation, Lavoisier, Paris, 1987.
[6] A. Bejan, Advanced Engineering Thermodynamics, 2nd Edition, Wiley, New York, 1997, pp. 376, 546.
[7] T.R. Strobridge, D.B. Chelton, Size and power requirements of 4.2 K refrigerators, Adv. Cryogenic Engrg. 12 (1967) 576–584.
[8] A. Bejan, M.R. Errera, Maximum power from a hot stream, Internat. J. Heat Mass Transfer 41 (1998) 2025–2036.
[9] P. Walsh, P. Fletcher, Gas Turbine Performance, Blackwell Science Ltd. and ASME, New York, 1998, pp. 78, 106, 138.
[10] J.E. Hesselgreaves, Rationalization of second law analysis of heat exchangers, Internat. J. Heat Mass Transfer 43 (2000) 4189–4204.